



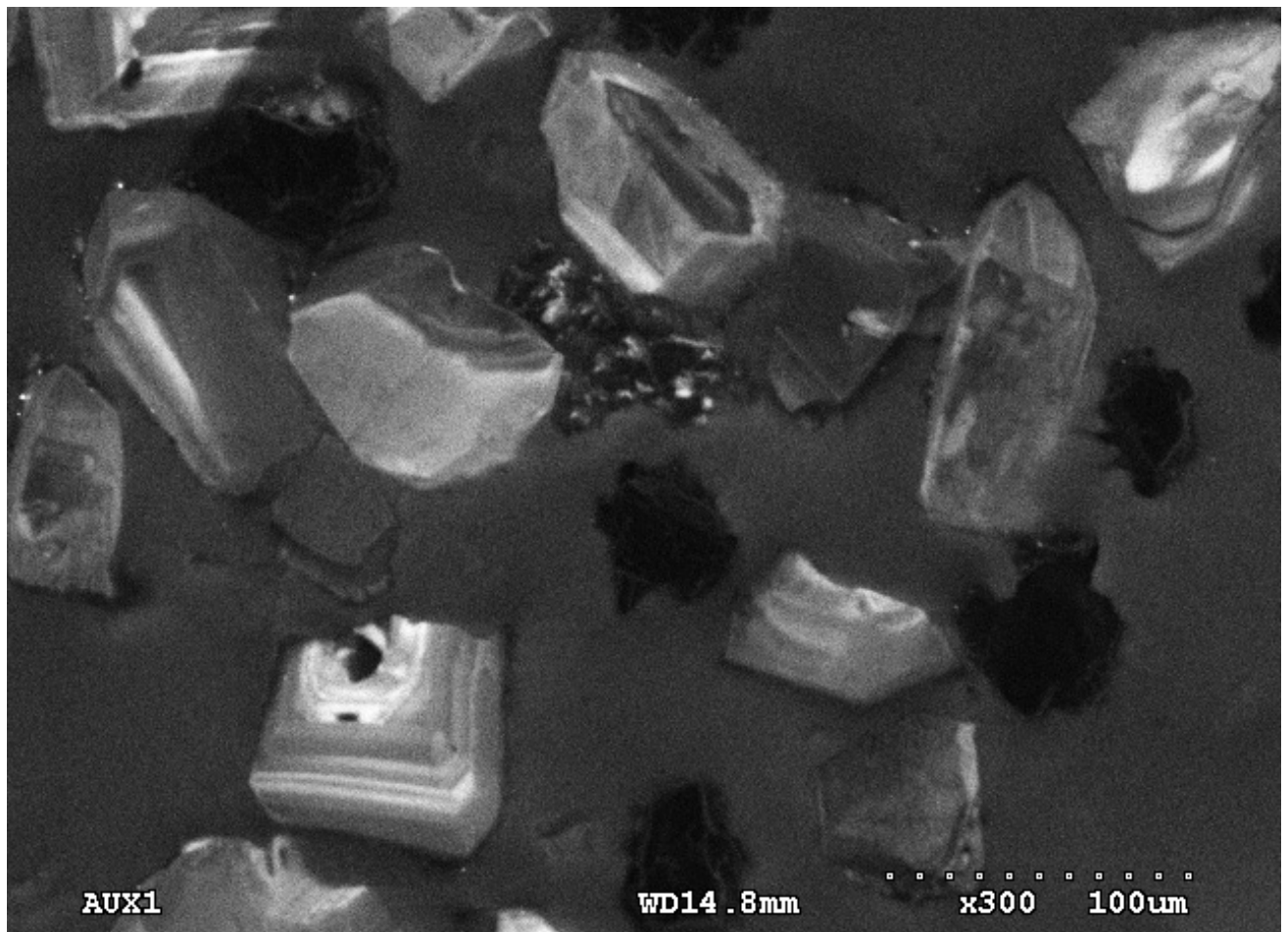
Stockholm
University

Bachelor Thesis

Degree Project in
Geology 15 hp

U-Pb zircon dating of igneous and detrital samples from the Thalbah Group in Saudi Arabia

Jonatan Olsson



Stockholm 2015

Department of Geological Sciences
Stockholm University
SE-106 91 Stockholm

Abstract

The provenance of a conglomerate from the Maatar formation of the Thalbah group in NW Saudi Arabia is investigated. Igneous clasts within the conglomerate preserve a record of magmatism related to the formation of the Arabian-Nubian Shield between 800 and 550 Ma ([Johnson et al., 2011](#)). U-Pb zircon dating via laser inductively coupled plasma was performed on a number of clast samples, together with their sandstone matrix. The clast gives ages of 653 ± 10 Ma, 710 ± 10 Ma and 753 ± 10 Ma. The matrix provides a range of ages from 405 Ma to 2600 Ma. All ages can be derived from locally derived sources and supports the hypothesis that the Thalbah group represents locally derived recycled material.

Table of contents

Abstract	1
Table of contents	3
1 Introduction	4
1.1 The Arabian-Nubian Shield and the Thalbah Group	4
1.2 Description of the Project	5
1.3 U-Pb dating and Zircons	6
1.4 LA-ICPMS and CL	6
2 Samples	7
3 Methods	9
3.1 Mechanical Separation	9
3.2 Heavy Liquid Separation	9
3.3 Sieving, Picking and Mounting	9
3.4 SEM and CL	10
3.5 Laser Ablation ICPMS	10
3.6 Analysis of Raw Data	10
4 Results	11
4.1 Sample Overview	11
4.2 CL Images	11
4.3 Igneous Clast Ages	12
4.4 Detrital and Metasedimentary Ages	13
5 Discussion	14
5.1 Implications of the Analytical Results	14
5.2 Comments on the quality of data	15
6 Acknowledgments	15
7 References	16
Appendix	17

1 Introduction

1.1 The Arabian-Nubian Shield and the Thalbah Group

The Arabian-Nubian Shield, ANS, is located on the African and Arabian plates and is divided into its Arabian and Nubian parts by the Red Sea (fig. 1). The ANS formed during a sequence of events involving the opening and closing of the Mozambique Sea and the formation of Gondwana (Johnson et al., 2011)

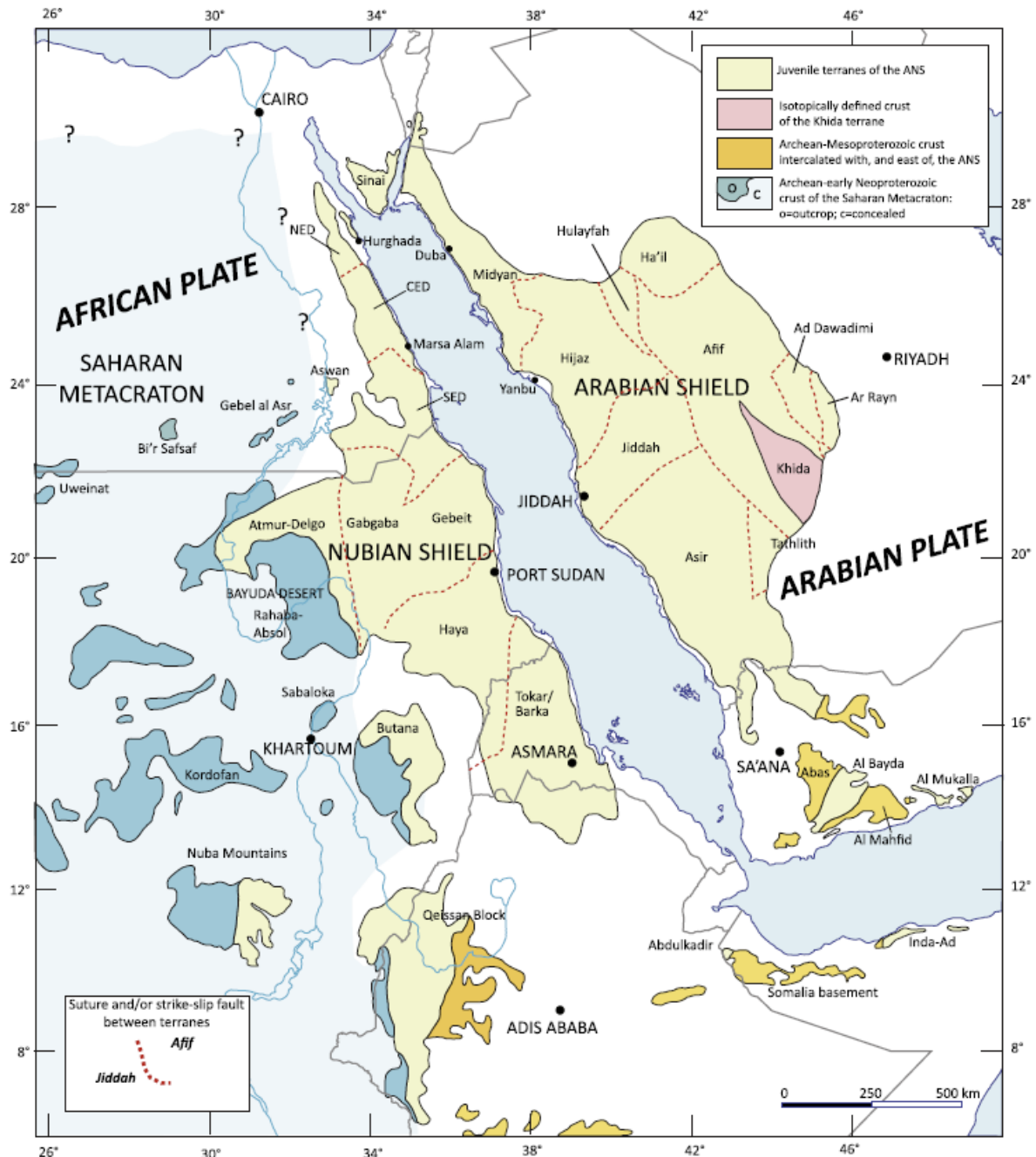


Figure 1. Map showing extent of the ANS. The Thalbah group that was investigated is located in the Midyan terrain in NE Saudi Arabia. The Hammamat group is located in the Eastern Desert in Egypt which is divided into a northern (NED), central (CED) and southern (SED) part. Image from Johnson et al, 2011.

The first stage in the formation of the ANS starts with the break-up of Rodinia which occurred between roughly 870-800 Ma (Johnson et al., 2011). During Rodinia's break-up the accompanied rifting will lead to the formation of the Mozambique Ocean and with it a system of arcs, back-arcs and ocean spreading zones (Pease et al., 2013). The arcs will ultimately accrete to the nearby Saharan Craton and form a region of amalgamated arcs, back-arc basins and oceanic crust and it is this collection of material that makes up the bulk of the ANS. The Mozambique Ocean will exist until 670 Ma at which time there is a collision between what will become the eastern and western parts of the new continent Gondwana and forms the East African Orogen (Johnson et al., 2011; Bezenjani et al., 2014). With this orogen there is also a transition from arc magmatism to the formation of large plutonic complexes within the ANS. The area continues to be tectonically active until 550 Ma, with ongoing magmatism and structural reworking due to the shortening during collision. At the end of orogen the area is highly eroded, becomes a region of low relief and a depositional site for Paleozoic sandstones (Johnson et al., 2011).

This Project involves samples taken from the Thalbah group which is located in the Midyan terrain in North-Western Saudi Arabia (fig. 1). There are two major formations in the Thalbah group; Dhaiqa and Maatar. The overlying Dhaiqa formation consists of calcareous sandstones and siltstones and is about 500 m thick (Pease., 2010). The exact depositional environment for the Dhaiqa formation is debated. There is evidence that it is aqueous but nothing that can unambiguously say if it is marine, lacustrine or estuarine. The Dhaiqa formation has a reported formation age of 600 to 530 Ma (Miller et al., 2008). Molassic sediments from the Maatar formation is underlying the Dhaiqa formation indicating that a change from a terrestrial to an aqueous environment occurred. The Maatar formation consists of a fining upwards sediments, from a conglomerate to a mudstone over about 150m (Pease., 2010). The Maatar formation has an equivalent on the Egyptian side of the red sea in the Hammamat group which also consists of molasse sediments (Bezenjani et al., 2014). There is debate regarding the formation history of the Hammamat group centered on the tectonic differences observed throughout the group making a single tectonic model difficult to achieve (Bezenjani et al., 2014).

1.2 Description of the Project

This project examines the relationship between the clasts in the Maatar formation conglomerate and their sandstone matrix in an attempt to provide insight on the formation history of the Thalbah group. The project is designed to determine the age of each of the igneous and metamorphic clasts and to assess how these ages are represented in the sandstone matrix. The matrix age populations will also be determined and evaluated for correlations with the magmatism associated with the formation of Gondwana (670-550 Ma) and the arc magmatism of the Mozambique Ocean (800-630 Ma) (Johnson et al., 2011). The ages of the grains present in the conglomerate will provide information about the relationship between the clast and the matrix and depending on those relations the sedimentological setting can be further understood. The hypothesis is that the conglomerate is made up of locally derived material that has been recycled. The dating is performed using the U-Pb technique on zircons from all samples and the analyses were performed using laser ablation inductively coupled mass spectrometry, LA-ICPMS, together with cathodoluminescence, CL, imaging.

1.3 U-Pb Dating and Zircons

Zircon ($ZrSiO_4$) is a naturally occurring accessory mineral that can be found in both igneous and sedimentary rocks, as well as in metamorphic rocks (Finsch et al., 2003). Zircons can incorporate a number of different trace elements in its structure. The mineral is very stable chemically as there is little element exchange after formation, and physically as the mineral itself tends to survive for a long time. It is consequently well suited for use as a dating tool in geochronology. Zircon has a density of 4.66 g/cm^3 which is relatively high and useful when separating it from other rock-forming minerals (Finsch et al., 2003).

Among the different trace elements that can be incorporated into the structure of zircon the elements of the U-Th-Pb system are the ones that are commonly used for dating purposes. The system involves 3 distinct decay reactions, shown with their decay constants (Winter., 2014) below.

- (1) $^{238}\text{U} \rightarrow ^{234}\text{U} \rightarrow ^{206}\text{Pb}$ ($\lambda=1.15512 \cdot 10^{-10} \text{ a}^{-1}$)
- (2) $^{235}\text{U} \rightarrow ^{207}\text{Pb}$ ($\lambda=9.8485 \cdot 10^{-10} \text{ a}^{-1}$)
- (3) $^{232}\text{Th} \rightarrow ^{208}\text{Pb}$ ($\lambda=4.9475 \cdot 10^{-11} \text{ a}^{-1}$)

From the decay constants of equations 1 and 2, the two decay chains will evolve independently and when looking at them together the value of $^{207}\text{Pb}/^{235}\text{U}$ will always be larger than $^{206}\text{Pb}/^{238}\text{U}$ because ^{235}U decays faster. As long as the system is closed and uninterrupted $^{207}\text{Pb}/^{235}\text{U}$ and $^{206}\text{Pb}/^{238}\text{U}$ will both be evolving along a curve called a Concordia. If the system is open it cannot be used for age determinations and (Winter., 2014).

1.4 LA-ICPMS and CL

Laser ablation techniques utilize a high energy laser beam focused at the surface of a target (the zircon grain in this case) to mobilize the atoms present in the sample. The laser will excite electrons in the sample and subsequently melt and vaporize the sample forming an aerosol (Kořler et al., 2003). The aerosol is then transported towards the inductively coupled plasma mass spectrometer, ICPMS, with the aid of a carrier gas, in this case Helium. A tiny cone above the sample location, an ablation cup, focuses the aerosol and thus ensures that more of the aerosol is collected.

In the ICPMS the aerosol is put through a torch made up of a coil that heats the sample. An Argon gas is introduced to the sample. In the torch a plasma forms due to the high temperatures (10,000K) and the Argon gas will start to lose electrons and thereby ionizing the aerosol and generating an ion beam. The ion beam is then directed into a vacuum chamber where a series of electrostatic lenses focus the beam and accelerate it towards the quadrupole. The quadrupole can be used with an alternating current (AC) or a direct current (DC) and so is able to direct ions with a specific weight and/or charge interval to the detector where the ions are counted and the information is then recorded by using software (Kořler et al., 2003).

Zircons often have a heterogeneous internal structure that is influenced by a number of different processes. These include: compositional zoning, different types of alteration (hydrothermal, etc.), dissolution as well as simple impurities (Nasdala et al., 2003). Using CL some structures can be observed. CL is a phenomenon where an electron beam focused on a surface (sample) will cause emission of photons from that surface and the wavelength of the light emitted will depend on the elements present (Nasdala et al., 2003). In the case of zircons, the varying amounts of REEs incorporated into the mineral will have an effect of the wavelength of the emitted photons and this makes it possible to see the internal structure of the grains. This is very useful when deciding where to analyse the grains so that areas with many impurities and chaotic internal structure can be avoided.

2 Samples

The seven samples (fig. 2) selected for this project are all from the Maatar formation conglomerate. The chosen samples represent six different sets of rounded clasts of different rock types, as well as the sandstone in which the clasts were embedded.

There are four different igneous clasts among the samples. Two of them are granitic (10d-1 and 12a), one of them is andesitic (10c), and one of them is finer grained volcanic clast (10b). 10c is a single clast broken into two pieces. One part of the clast contains a small part of the metasedimentary which may introduce some contamination and influence the final result. The granitic sample 12a was already pre-crushed and the description of how the other samples were crushed does not apply to it.

There are two different metamorphic clasts among the samples: one hydrothermal (10d-2) and one metasediment (12b). The hydrothermal sample shows high degree of alteration which could make it difficult to date. The metasedimentary clast is a compacted conglomerate with small pebbles and smaller grains in a fine matrix. Because of its sedimentary nature the metasediment will be treated the same way as a detrital sample, that is looking at populations of different grains ages instead of determining a formation age. The final sample (32) is the sandstone matrix hosting all the clasts. A short overview of all samples is provided in table 1 in the results section.



Figure 2. Images of the samples. In order: 10b Volcanic clast, 10c Andesitic clast, 10d-1 Granitic clast, 10d-2 Hydrothermal altered metamorphic clast, 12b Metasediment, 32 Sandstone. There is no image of sample 12a Granitic clast.

3 Methods

3.1 Mechanical Separation

The process of reducing whole rock samples down to a few grains of zircon to be analyzed by the LA-ICPMS is performed in multiple stages using a number of different techniques.

The first stage is crushing the rock to sand size particles. This was performed using a *Retsch RS 200* vibratory disc mill. The mill is only able to handle rock pieces of about 1 cm³ so the rock samples had to be cut and hammered until they were sufficiently small to feed into the mill. During this process thin slices of the rocks are cut and preserved for identification of the different rock types (see [fig. 2](#)) since they were heavily weathered and hard to identify without a fresh surface. Thin-sections were not made due to limited sample size and time limitation but would have provided a more accurate classification of the rocks.

The first stage of actual separation was with a Wilfley-table. The Wilfley-table utilizes flowing water to separate grains, similar to how a river works. The lighter grains are more readily transported by the water and move faster, leaving the heavy fraction (which includes zircon) behind. The Wilfley-table reduces the sample to a tiny fraction of its original size. A magnet is then used on the heavy fraction to remove magnetic phases from the samples.

3.2 Heavy Liquid Separation

The high density of zircon allows further separation of the heavy fraction. The synthetic liquid methylene iodide, ML, (also known as diiodomethane) has a density of about 3.3 g/ml. The method uses a separating funnel filled with enough ML to accommodate the sample and when the sample is introduced the particles lighter than the ML float on top of the liquid while the heavy particles sink to the bottom. The two fractions are then removed from the ML and thoroughly cleaned with acetone so the ML would not interfere with any analysis. During this process the samples are reduced to about half their size compared to before the heavy liquid separation.

3.3 Sieving, Picking and Mounting

After looking at the different samples in a binocular microscope the decision was made sieve two of the samples. The samples 32 and 12a were sieved with sieve openings of 163µm and 130µm respectively. The zircons in both samples were generally smaller than the other grains so sieving efficiently increased the relative abundance of zircon in preparation for picking.

Individual zircons were then hand-picked with the help of a light microscope. Two different methods were used when picking: for the igneous clasts only zircons of the most dominant type were picked, since they would give the best estimate of the formation age. At least 50 grains were picked for the igneous clasts. For the detrital and metasedimentary samples the approach was to try and pick zircons from all the different populations present in the sample; this meant also trying to find zircons from outside the dominant group and achieving a representative selection of the sample. This

process is prone to some bias since it is done by visual identification of grains and populations in the sample. At least 150 grains were picked for the detrital and metasedimentary samples.

The picked grains were placed on tape. When all samples were picked a plastic mounts was made trapping the grains and making it possible to polish the mount and grains using a diamond spray until the grain cores were exposed. The surface of the mount was then coated with a thin gold layer before imaging.

3.4 SEM and CL

Images were made of the different samples to determine which grains were suitable for analysis. A *Hitachi S-4300* scanning electron microscope, SEM, with cathodoluminescence, CL, detector at the Swedish Museum of Natural History was used. Comprehensive CL and SEM images were made of all samples. The instrument was set to an accelerating voltage of 15.0 kV and a beam current of 10 μ A. After the CL imaging 5 of the 7 original samples were selected to be further analyzed by LA-ICPMS.

3.5 Laser Ablation ICPMS

The analysis of the samples was made with a *New Wave NWR 193nm Excimer* laser coupled to a *Thermo X-series 2* quadrupole inductively coupled plasma mass spectrometer, ICPMS. The laser was set to a laser energy density of 7 J/cm², a repetition rate of 10 Hz and a spot size 25 μ m. For each grain analyzed the same analytical sequence was used: background for 15 seconds, then measurement while the laser was ablating for 40 seconds, and then a 10 second washout before moving to the next grain. For accuracy control a known standard (the so-called secondary standard) was analyzed and its results evaluated against the expected value for the standard. The standard used was FC-5z. Plesovice was used as the primary calibration standard. An analysis of both Plesovice and FC-5z was made for every 10 grains of the sample as well as a few times the beginning of each analytical session.

3.6 Analysis of Raw Data

The data received from the ICPMS is processed in the program *Iolite* run within the *IGOR PRO* environment. The program looks at the relative abundances of the different U and Pb isotopes and calculates ages using this data. Before ages are calculated the background was removed and downhole fractionation were made (to account for the slight variation in values as the laser drills into the zircon (Kořler et al., 2003)). The secondary standard (FC-5z) gives ages within error of its known age indicating that the ICPMS working well.

After being processed in *Iolite* the data was exported into *Excel* where the application *Isoplot* is used to determine the final ages from analyses with a discordance of 10% or less. The igneous grains were plotted on a concordia diagram to calculate a single Concordia age. The ages for detrital and metasedimentary samples were plotted on a histogram with bins corresponding to 4 σ error based on the average error for the entire sample rock using the errors for all ages used in the plot. The bins size

used was 54 Ma for sample 32 and 56 Ma for sample 12b. A curve was plotted for each histogram which gives the grain distribution.

4 Results

4.1 Sample Overview

A sample summary is given in [table 1](#) and as can be seen only a small amount of the igneous grains were analyzed. The number of grains analyzed will have an impact on the quality of the data but, since only a single age is required if the grains match an age can be obtained even with so few analyses. The amount of grains analyzed in the detrital and metasedimentary samples (>125) match what is required for having at least a 95% probability of finding grains from each population present in the samples ([Fedo et al., 2003](#)).

TABLE 1

SAMPLE NAME	TYPE	GRAINS PICKED	GRAINS ANALYSED	NOTES
10B	Volcanic clast	50	None	
10C	Andesitic clast	50	8	2 pieces
10D-1	Granitic clast	50	5	
10D-2	Hydrothermal clast	50	None	
12A	Granitic clast	50	21	Received already crushed
12B	Metasedimentary clast	150	150	
32	Sandstone	150	150	Matrix

4.2 CL images

The CL imaging shows a clear internal structure of the zircon grains and makes it easy to distinguish them from grains of other minerals. An example of a CL image from sample 12b is provided together with the calculated ages of the grains in the image ([fig. 3](#)).

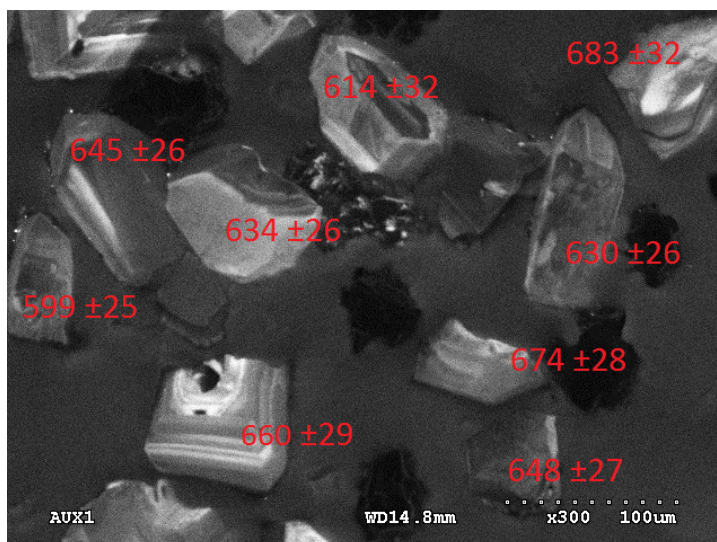


Figure 3. CL image of grains from sample 12b with their respective ages and 2σ error.

4.3 Igneous Clast Ages

The ages determined for the igneous clasts are displayed in figure 4. The graphs show the final age for each analyzed grain plotted together on a concordia diagram with the theoretical concordia curve shown. Sample 12a shows inheritance of xenocrystic zircons as well as lead loss. These analyses were excluded from the final analysis and only the youngest concordant grains were used in the age determination for this sample. The samples give final ages of 710 ± 10 (10c), 753 ± 10 (10d-1) and 653 ± 10 Ma (12a); all of these are reasonable in regards to the known history of the ANS.

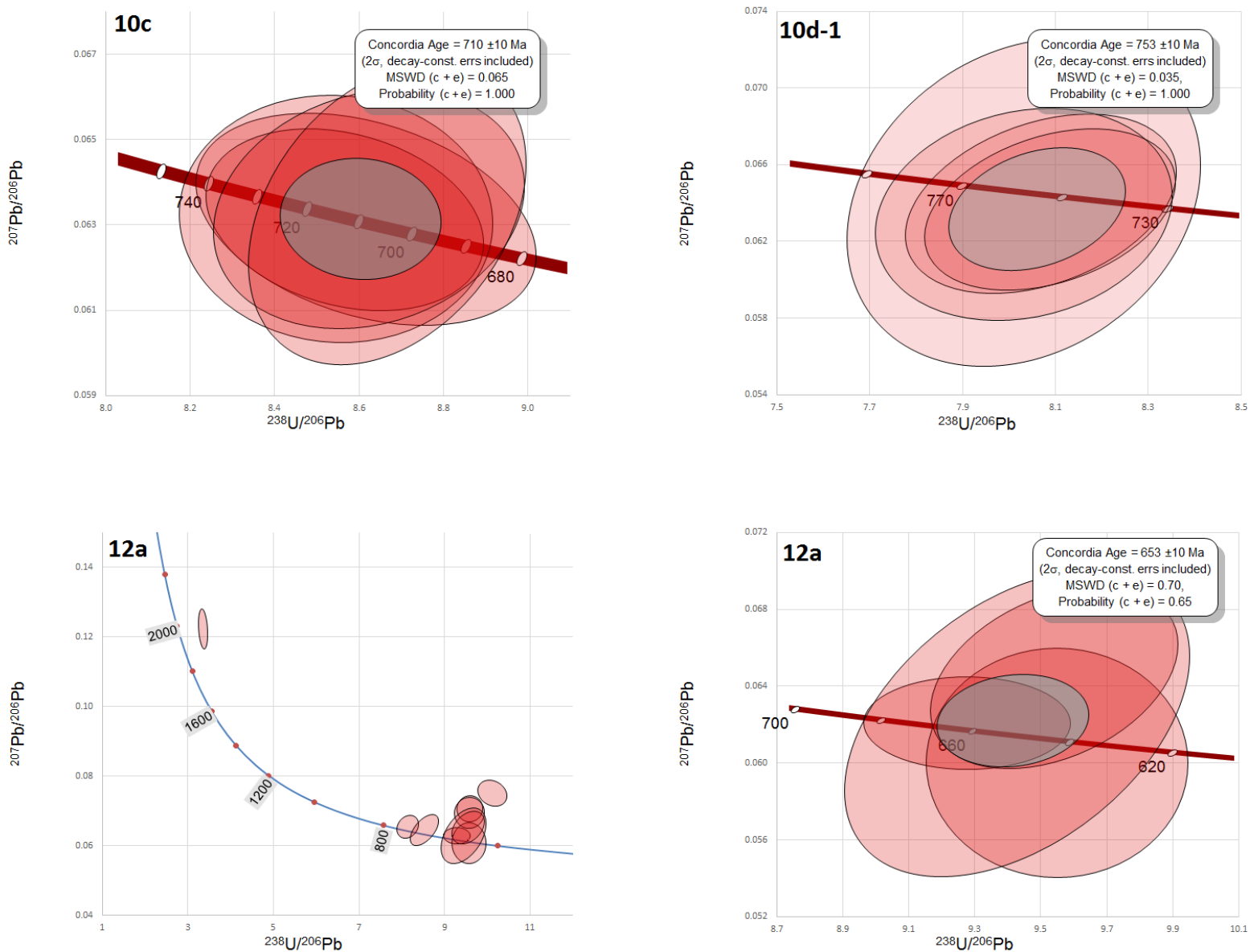


Figure 4. Final calculated ages for the 3 analyzed igneous clast. The final age with its 2σ error is represented by a gray ellipse. The given values for the analyzed grains with their 2σ are displayed as red ellipses. Sample 12a is shown in two separate plots due to the big spread. The first plots displays all grains, the second shows the youngest concordant grains which were also used to calculate an age for the clast.

4.4 Detrital and Metasedimentary Ages

The detrital sample (32) is shown in figure 5 a number of different age populations can be recognized in the sample. The youngest population plots with a peak at 405 Ma which is significantly younger than the 600 Ma that has been reported for this unit (Miller et al., 2008; Bezenjani et al., 2014). The peak represents 5 analyses and is therefore robust. There are some grains that are as old as 2600 Ma and an intermediate population around 1900 Ma. Most of the grains plot between 550 and 800 which corresponds to the magmatic activity associated with the opening of the Mozambique Ocean and the East African Orogen. The ages from the igneous clasts each defines one of the three peaks in figure 5. Sample 12a (653 ± 10 Ma) could correspond to the peak at 664 Ma; sample 10c (710 ± 10 Ma) could correspond to the peak at 715 Ma and sample 10d-1 (753 ± 10 Ma) has the peak at 766 Ma within its error margin. The relative height of the peaks does not necessarily signify a higher amount of the different populations because of the methods used (bias in picking grains, etc.) but does reflect the populations that are present. The peak at 405 Ma suggest a maximal depositional age at ~ 405 Ma.

The metasedimentary sample (12b) is plotted in figure 6 in the same way as the detrital but as can be seen the variation in the ages of the grains is not as diverse. The ages of the grains range from 750 to 550 Ma and this is a great match with the magmatic and tectonic history of the region, suggesting deposition after 550 Ma. All of the ages in sample 12b also fit within the populations present in sample 32.

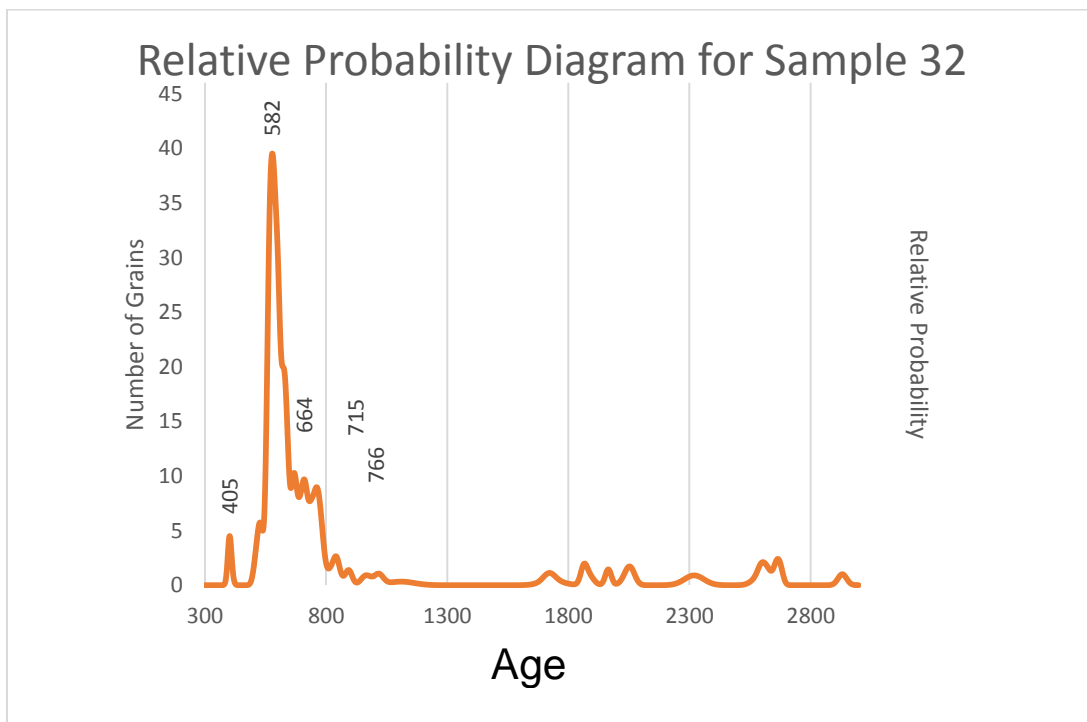


Figure 5. Probability diagram for the Sandstone matrix (sample 32). The graph shows the distribution of ages for the dated zircons. Interesting peaks are defined with the age at which the peak occurs.

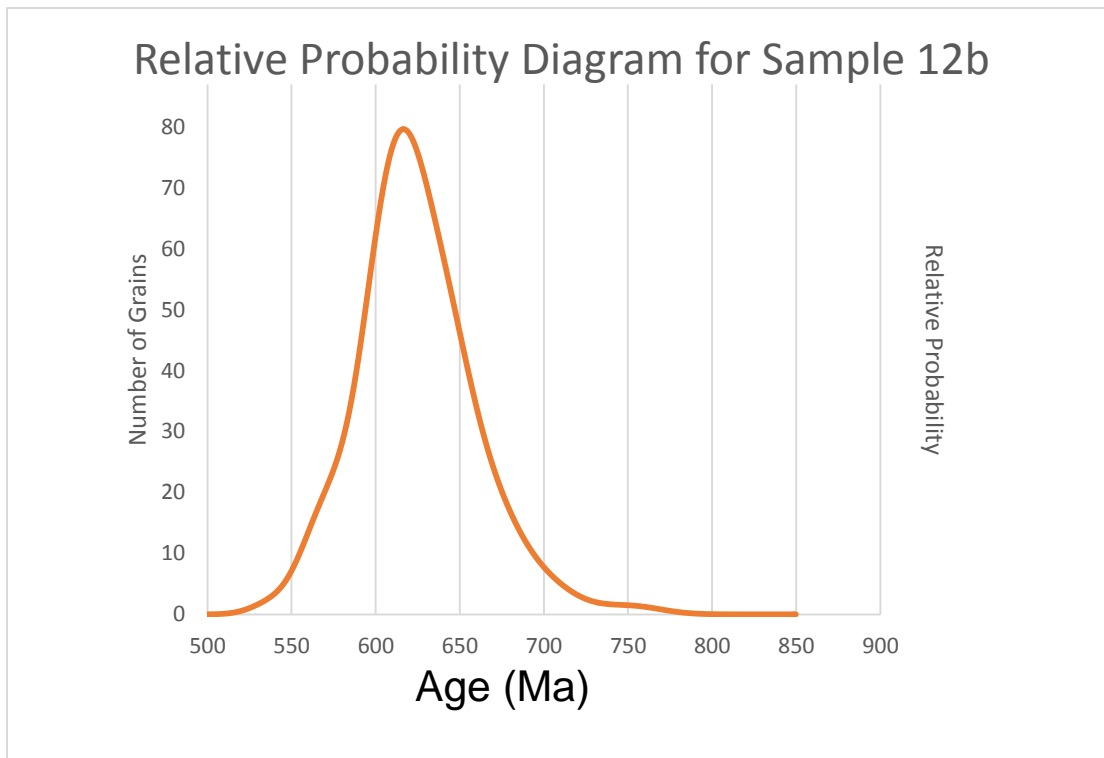


Figure 6. Probability diagram for the metasediment (sample 12b). The graph shows the distribution of ages for the dated zircons. All grains fall within a single region ranging from 550 to 750 Ma.

5 Discussion

5.1 Implications of the Analytical Results

The data generated in this project provides new insight into the formation history of the Thalbah group. The young, 405 Ma, population of grains found in detrital sample (32) highlights the possibility that the formation age of the Maatar formation is younger than previously been proposed by Bezenjani and Miller. Miller reported grains of zircon as young as 599 ± 4.8 Ma in the overlying Dhaiqa formation (Miller et al., 2008) and a basal layer with younger age seems counterintuitive. However mapping in the region is poor and the unit may be mis-identified.

The Maatar formation represents molasse sediments and contains large clasts; this suggests deposition close to the source of the detrius. The metasedimentary clast (12b), made up of grains from a period when the ANS was tectonically active, indicates previous deposition and that the material was compacted; this must have formed after 550 Ma (based on the youngest population of grains) and then been broken up and transported into what would to become the Maatar formation. The sedimentary portion on the 10c igneous sample supports the same process and it is likely that the clast has previously been part of another (or the same as 12b) compacted conglomerate that has been transported to the Maatar formation. During this time the depositional basin would have received the young grains as well, though their origin would not be associated with the formation of the ANS as described by Johnson (Johnson et al., 2011). After molasse deposition the basin changed character and became an aqueous depositional environment (Miller et al., 2008); during this

transition it was possible that the source of the material also changed, i.e. the Dhaiqa formation also received recycled material but from locations with a slightly different formation age. The involvement of water makes it possible for the basin to receive material from further away and supports this argument.

There is a possibility that the grains with very young ages could be due to contamination, although the probability of multiple grains of similar age contaminating the sample would be very small. In the case of a contamination second youngest population would have ages around 550 Ma and this would match with the suggested youngest age of the Dhaiqa formation proposed by Miller which is ~530 Ma (Miller et al., 2008). This would not make the argument for recycled sediments less valid but would change the timing back to the end of the East African Orogen.

5.2 Comments on the Quality of Data

The low amount of grains analyzed on the igneous clast limits the use of the data, but within the confines of the project the fact that all the ages match with previously dated rocks in the region. Ages present in the detrital and metasedimentary sample makes it probable that these samples give reasonable ages despite the low total number of grains analysed. Sample 32 and 12b have enough grains to make the results valid and with a 95% probability of finding all populations (Nasdala et al., 2003) and nothing in the values suggest any issues with the data.

The 405 Ma population is significantly different than previously reported values and changes the way how the Thalbah group must be viewed. The likelihood of it being contaminated is regarded as low, and the discrepancy from what is previously reported must be considered. To conclude, the Thalbah group must have formed after 405 Ma and another experiment should be made to support the validity of this age for the part of the Maatar formation.

6 Acknowledgements

I would like to thank the following people for aiding me in this project: Victoria Pease for supervising and guiding me in this project; Cora Wohlgemuth-Ueberwasser for introducing me to and aiding me with the SEM, LA-ICPMS and Wilfley-table; Dan Zetterberg for assistance with crushing the rock samples; Runa Jacobsson for introduction to the heavy liquid separation; Mira Rundberg for donating a strain of hair used for picking zircons.

7 References

- Johnson, S.A., Andersen, A., Collins, A.S., Fowler, A.R., Fritz, H., Ghebreab, W., Kusky, T., Stern, R.J. (2011) 'Late Cryogenian–Ediacaran history of the Arabian–Nubian Shield: A review of depositional, plutonic, structural, and tectonic events in the closing stages of the northern East African Orogen', *Journal of African Earth Sciences*, 61(1), pp. 167-232.
- Pease, V., Johnson, P.R. (2013) 'Introduction to the JEBEL volume of Precambrian Research', *Precambrian Research*, 239, pp. 1-5.
- Nasiri Bezenjani, R., Pease, V., Whitehouse, M.J., Shalaby, M.H., Kadi, K.A., Kozdroj, W. (2014) 'Detrital zircon geochronology and provenance of the Neoproterozoic Hammamat Group (Igla Basin), Egypt and the Thalbah Group, NW Saudi Arabia: Implications for regional collision tectonics', *Precambrian Research*, 245, pp. 225-243.
- Pease, V. (2010) 'JEBEL Project October 2009 field excursion to the Midyan terrain, Kingdom of Saudi Arabia', *Saudi Geological Survey Technical Report*, 2, pp. 28-31.
- Miller, N., Johnson, P.R., Stern, R.J. (2008) 'Marine versus non-marine environments for the Jibalah group, NW Arabian Shield: A sedimentologic and geochemical survey and report of possible metazoan in the Dhaiqa formation', *Arabian Journal for Science & Engineering*, 33(1C), pp. 55-77.
- Finch, R.J., Hanchar, J.M. (2003) 'Structure and chemistry of zircon and zircon-group minerals', *Review in Mineralogy & Geochemistry*, 53, pp. 1-25.
- Winter, J.D. (2014) *Principles of igneous and metamorphic petrology*, 2nd edn., Harlow, UK: Pearson Education Limited
- Košler, J., Sylvester, P.J. (2003) 'Present trends and the future of zircon geochronology: Laser ablation ICPMS', *Review in Mineralogy & Geochemistry*, 53, pp. 243-271.
- Nasdala, L., Zhang, M., Kempe, U., Gaft, M., Andrut, M., Plötze, M. (2003) 'Spectroscopic methods applied to zircon', *Review in Mineralogy & Geochemistry*, 53, pp. 427-467.

8 Appendix

The following table shows the comprehensive list of all analysis made in the LA-ICPMS. Values not used in the final calculation of ages are stricken in the list and no ages are given when the discordance is higher than 10%. The list shows the concentration of measured U, Th and Pb together with the 3 main isotopic relations that are used when calculation ages. The ages provided where calculated the $^{206}\text{Pb}/^{238}\text{U}$ ratio for ages under 1 Ga and the ratio between $^{207}\text{Pb}/^{206}\text{Pb}$ was used for ages older than 1 Ga. The 2σ errors are provided for all ratios as well as the final age and for each grain the final discordance percent is displayed.

TABLE 2

Sample /spot #	[U] ppm	[Th] ppm	[Pb] ppm	$^{207}\text{Pb}/$ ^{235}U $\pm 2\sigma$	$^{238}\text{U}/$ ^{206}Pb $\pm 2\sigma$	$^{207}\text{Pb}/$ ^{206}Pb $\pm 2\sigma$	Disc %	Final Age	$\pm 2\sigma$			
10c-1	104	7	8	1.050	0.1	0.119	0.006	0.0637	0.006	7	726	32
10c-3	493	41	51	1.011	0.06	0.116	0.005	0.0633	0.003	5	709	26
10c-5	786	68	78	1.017	0.05	0.117	0.004	0.064	0.002	4	712	22
10c-6	705	61	71	1.020	0.06	0.117	0.004	0.0647	0.003	3	714	25
10c-7	739	66	68	1.014	0.05	0.116	0.004	0.0648	0.003	3	708	24
10c-11	3933	932	911	1.600	0.54	0.076	0.025	0.1529	0.005	53		
10c-12	176	95	32	1.024	0.1	0.096	0.006	0.0771	0.005	13		
10c-14	674	63	75	1.007	0.05	0.116	0.004	0.065	0.003	5	704	21
10d-1-1	44	27	28	1.100	0.12	0.125	0.005	0.066	0.007	10	757	28
10d-1-3	62	38	41	1.094	0.06	0.124	0.004	0.0654	0.004	9	754	22
10d-1-6	206	163	148	1.086	0.06	0.124	0.004	0.0649	0.003	6	753	20
10d-1-8	73	40	37	1.089	0.08	0.125	0.004	0.064	0.004	7	757	24
10d-1-11	49	18	19	1.104	0.08	0.125	0.004	0.0647	0.005	12		
12a-1	975	288	296	1.008	0.05	0.105	0.003	0.069	0.003	7	641	16
12a-2	1465	1960	1695	0.924	0.04	0.108	0.003	0.0622	0.002	3	661	18
12a-3	104	813	667	1.440	0.18	0.102	0.007	0.107	0.01	32		
12a-4	50	410	353	0.866	0.08	0.105	0.004	0.0603	0.005	10	642	21
12a-5	57	445	382	0.875	0.09	0.102	0.003	0.062	0.006	12		
12a-6	87	166	157	1.357	0.09	0.104	0.003	0.094	0.006	23		
12a-7	189	440	493	2.160	0.42	0.146	0.009	0.12	0.026	28		
12a-9	1301	870	927	1.173	0.1	0.103	0.003	0.0801	0.006	16		
12a-10	87	583	543	1.023	0.07	0.104	0.003	0.0728	0.005	11		
12a-12	373	319	363	1.105	0.05	0.124	0.003	0.0649	0.002	5	753	19

12a-13	110	795	810	1.510	0.11	0.104	0.004	0.106	0.007	29		
12a-14	486	724	796	1.103	0.06	0.107	0.004	0.0757	0.004	11		
12a-15	1056	518	668	0.992	0.06	0.105	0.003	0.0676	0.003	5	641	18
12a-16	55	678	719	1.226	0.08	0.102	0.003	0.0862	0.005	18		
12a-17	489	3048	3038	0.932	0.05	0.105	0.004	0.0634	0.004	5	643	20
12a-18	90	846	837	0.908	0.09	0.106	0.005	0.0634	0.007	9	650	29
12a-19	1670	4263	4923	1.016	0.06	0.099	0.003	0.0739	0.003	10		
12a-20	217	160	600	5.350	0.29	0.317	0.009	0.1211	0.005	7	1774	45
12a-21	513	830	923	1.036	0.05	0.118	0.004	0.0642	0.003	5	718	23
12a-22	117	963	985	1.040	0.14	0.104	0.004	0.0736	0.009	13		
12a-23	2869	2915	2921	0.931	0.04	0.109	0.004	0.062	0.002	3	667	21
12b-1	380	99	187	0.790	0.06	0.096	0.004	0.0607	0.003	5	592	25
12b-2	260	81	123	0.765	0.07	0.093	0.004	0.0604	0.005	9	575	25
12b-3	411	63	123	0.780	0.06	0.095	0.005	0.0606	0.004	5	587	27
12b-4	345	98	165	0.814	0.06	0.099	0.004	0.0611	0.003	6	607	25
12b-5	325	60	105	0.761	0.06	0.094	0.004	0.0604	0.004	7	577	24
12b-6	214	83	151	0.768	0.08	0.093	0.004	0.0605	0.005	10	573	25
12b-7	704	175	298	0.749	0.06	0.091	0.004	0.0612	0.003	4	564	24
12b-8	253	42	66	0.802	0.08	0.098	0.005	0.0601	0.006	8	602	28
12b-9	484	82	144	0.754	0.05	0.093	0.004	0.0605	0.003	5	571	24
12b-11	211	82	80	0.750	0.07	0.092	0.005	0.0596	0.005	10	567	26
12b-12	269	93	84	0.790	0.11	0.095	0.005	0.0605	0.007	8	587	30
12b-13	351	161	129	0.762	0.08	0.091	0.005	0.0632	0.007	7	562	26
12b-14	145	72	75	0.900	0.11	0.106	0.005	0.0634	0.007	12		
12b-15	2018	705	535	0.763	0.05	0.094	0.004	0.0597	0.002	3	579	23
12b-16	1578	714	365	0.731	0.05	0.090	0.004	0.0594	0.002	3	557	24
12b-17	245	107	75	0.924	0.1	0.107	0.006	0.0623	0.005	9	657	33
12b-18	571	368	205	0.744	0.05	0.091	0.004	0.0602	0.003	6	561	24
12b-19	594	478	280	0.799	0.06	0.098	0.004	0.0603	0.003	4	600	25
12b-20	169	106	65	0.842	0.08	0.102	0.005	0.0587	0.004	10	623	29
12b-21	234	212	123	0.765	0.07	0.092	0.004	0.0608	0.004	9	569	24
12b-22	715	362	233	0.832	0.07	0.099	0.004	0.0622	0.004	7	607	25
12b-23	123	92	56	0.870	0.14	0.106	0.006	0.0607	0.009	11		
12b-24	177	106	59	0.710	0.06	0.088	0.004	0.0594	0.004	11		
12b-25	408	227	173	0.865	0.07	0.104	0.005	0.0624	0.004	4	636	27
12b-26	560	292	202	0.824	0.06	0.101	0.004	0.0593	0.003	6	618	26
12b-27	224	81	63	0.820	0.11	0.101	0.005	0.0595	0.007	8	619	32
12b-28	939	347	266	0.816	0.06	0.098	0.005	0.0613	0.003	4	601	27
12b-29	149	86	73	0.830	0.07	0.101	0.005	0.0615	0.004	9	618	27

12b-30	523	180	156	0.860	0.06	0.103	0.004	0.0618	0.003	4	634	26
12b-31	386	94	104	0.822	0.06	0.098	0.005	0.0631	0.004	7	604	27
12b-32	276	116	129	0.832	0.06	0.101	0.005	0.0623	0.003	6	623	27
12b-33	423	100	127	0.890	0.06	0.107	0.005	0.0607	0.003	5	655	28
12b-34	225	66	75	0.905	0.08	0.107	0.005	0.0636	0.005	6	661	28
12b-35	489	87	112	0.908	0.08	0.106	0.005	0.0634	0.004	6	650	30
12b-36	179	69	78	0.911	0.09	0.107	0.006	0.0643	0.006	10	657	33
12b-37	225	96	112	0.849	0.1	0.103	0.006	0.0611	0.007	9	633	34
12b-38	207	60	67	0.822	0.07	0.100	0.005	0.0585	0.004	9	614	28
12b-39	445	59	65	0.828	0.08	0.098	0.005	0.0618	0.005	11		
12b-40	211	56	64	0.809	0.07	0.098	0.004	0.0597	0.004	9	599	26
12b-41	557	165	147	0.807	0.06	0.097	0.004	0.0598	0.003	5	597	24
12b-42	260	112	107	0.852	0.06	0.102	0.004	0.0604	0.003	7	625	26
12b-43	519	175	178	0.880	0.06	0.105	0.005	0.0609	0.003	6	644	28
12b-44	282	114	97	0.822	0.08	0.098	0.005	0.06	0.005	7	605	26
12b-45	176	97	91	0.857	0.09	0.102	0.005	0.0579	0.005	9	627	29
12b-46	2150	654	497	0.838	0.06	0.100	0.005	0.0602	0.003	5	613	28
12b-47	251	99	78	0.855	0.07	0.101	0.005	0.0614	0.005	5	622	32
12b-48	2663	788	610	0.875	0.07	0.104	0.006	0.0606	0.003	3	640	32
12b-49	235	93	85	0.961	0.08	0.110	0.006	0.0637	0.004	6	678	33
12b-50	696	255	192	0.840	0.06	0.100	0.004	0.0603	0.003	4	615	25
12b-51	258	140	110	0.830	0.12	0.099	0.006	0.0628	0.007	7	609	32
12b-52	520	183	144	0.839	0.06	0.100	0.004	0.0609	0.003	5	613	26
12b-53	201	89	77	0.940	0.11	0.109	0.006	0.0632	0.007	7	666	36
12b-54	926	360	332	0.857	0.07	0.102	0.007	0.0617	0.005	8	625	39
12b-55	232	60	58	0.850	0.07	0.102	0.005	0.0613	0.004	5	627	31
12b-56	642	158	137	0.797	0.05	0.097	0.004	0.0599	0.003	5	597	24
12b-57	2566	819	670	0.842	0.06	0.100	0.004	0.0618	0.002	3	616	25
12b-58	479	131	98	0.821	0.06	0.101	0.005	0.0598	0.004	5	617	27
12b-59	186	87	82	0.831	0.08	0.099	0.006	0.061	0.005	8	609	33
12b-60	737	274	174	0.851	0.07	0.101	0.005	0.0624	0.004	5	620	30
12b-61	715	196	182	0.836	0.06	0.100	0.005	0.0611	0.003	5	614	26
12b-62	194	64	72	0.886	0.07	0.105	0.005	0.0614	0.003	7	645	29
12b-63	2894	804	771	1.019	0.07	0.116	0.007	0.064	0.003	4	708	38
12b-64	458	132	129	0.867	0.06	0.103	0.005	0.0625	0.003	7	629	26
12b-65	631	109	116	0.815	0.07	0.098	0.005	0.0612	0.003	4	602	27
12b-66	389	109	104	0.832	0.06	0.099	0.004	0.0616	0.003	7	609	25
12b-67	165	92	85	0.790	0.12	0.095	0.005	0.0599	0.008	8	584	28
12b-68	546	111	103	0.849	0.06	0.102	0.004	0.0613	0.003	5	626	25
12b-69	96	38	39	0.877	0.1	0.102	0.005	0.0636	0.006	14		

12b-70	762	324	322	0.843	0.06	0.101	0.004	0.0599	0.003	6	620	25
12b-71	724	147	165	0.885	0.07	0.105	0.005	0.059	0.004	5	645	27
12b-72	224	86	103	0.890	0.12	0.103	0.005	0.0616	0.008	10	634	31
12b-73	321	65	78	0.844	0.08	0.101	0.005	0.0603	0.005	7	620	30
12b-74	465	161	176	1.037	0.08	0.105	0.004	0.0713	0.004	10	641	26
12b-75	370	99	121	0.824	0.07	0.098	0.004	0.0594	0.004	8	602	25
12b-76	2010	1126	1421	1.106	0.09	0.124	0.006	0.0636	0.003	4	754	34
12b-77	182	51	78	1.001	0.08	0.115	0.005	0.0614	0.004	9	700	31
12b-78	169	50	70	0.874	0.07	0.103	0.005	0.0617	0.004	9	631	27
12b-79	308	60	111	0.960	0.1	0.112	0.007	0.0632	0.006	7	681	39
12b-80	510	86	124	0.890	0.06	0.104	0.005	0.0616	0.003	5	639	27
12b-81	668	112	156	0.835	0.06	0.099	0.004	0.0613	0.003	5	611	25
12b-82	509	91	119	0.823	0.07	0.099	0.004	0.0606	0.004	5	610	26
12b-83	477	115	160	0.860	0.06	0.103	0.004	0.0605	0.003	5	632	26
12b-84	448	85	103	0.886	0.07	0.104	0.005	0.0633	0.003	5	639	27
12b-85	420	116	134	0.850	0.09	0.102	0.005	0.0585	0.007	5	624	30
12b-86	131	41	61	0.881	0.08	0.104	0.005	0.0617	0.005	10	640	28
12b-87	233	71	80	0.870	0.1	0.103	0.005	0.0613	0.006	8	629	29
12b-88	600	105	138	0.848	0.07	0.100	0.005	0.0624	0.004	4	614	32
12b-89	128	23	32	0.940	0.1	0.110	0.005	0.0626	0.006	9	671	30
12b-90	631	122	155	0.882	0.06	0.104	0.005	0.0628	0.003	4	639	26
12b-91	962	395	300	0.854	0.06	0.101	0.004	0.0621	0.003	4	622	25
12b-92	3522	4281	2821	0.940	0.09	0.109	0.01	0.0624	0.003	5	669	57
12b-93	1119	439	331	0.910	0.07	0.107	0.005	0.0618	0.003	4	653	27
12b-94	131	67	58	0.928	0.09	0.109	0.006	0.0632	0.005	11		
12b-95	453	250	185	0.871	0.06	0.105	0.004	0.0606	0.003	6	641	26
12b-96	312	302	198	0.835	0.07	0.099	0.004	0.061	0.004	7	608	25
12b-97	516	245	184	0.875	0.07	0.103	0.005	0.0605	0.004	6	632	29
12b-98	843	343	274	0.913	0.09	0.106	0.005	0.0621	0.006	5	651	29
12b-99	92	67	46	0.940	0.12	0.111	0.006	0.061	0.007	9	679	35
12b-100	1024	1025	620	0.811	0.06	0.098	0.005	0.0597	0.003	4	600	26
12b-101	1434	634	421	0.839	0.06	0.100	0.005	0.0592	0.002	3	615	26
12b-103	179	115	94	0.953	0.08	0.111	0.005	0.06	0.004	8	677	29
12b-104	591	333	237	0.893	0.09	0.105	0.005	0.0616	0.004	5	642	29
12b-105	525	217	185	0.940	0.12	0.109	0.006	0.0639	0.006	6	668	35
12b-106	801	429	365	0.911	0.07	0.107	0.006	0.0603	0.004	5	655	33
12b-107	203	119	127	1.080	0.15	0.118	0.009	0.0625	0.009	9	718	52
12b-108	595	223	187	0.889	0.07	0.105	0.005	0.0605	0.003	5	643	27
12b-109	1599	485	379	0.810	0.06	0.097	0.004	0.0598	0.003	3	599	25
12b-110	492	394	349	0.899	0.07	0.105	0.005	0.0611	0.003	7	645	26

12b-111	622	599	494	0.875	0.06	0.103	0.004	0.0617	0.003	5	634	26
12b-112	140	68	60	0.927	0.08	0.108	0.005	0.0624	0.004	10	660	29
12b-113	256	146	130	0.948	0.07	0.110	0.005	0.0627	0.004	7	674	28
12b-114	2300	966	816	0.903	0.06	0.106	0.005	0.0625	0.003	3	648	27
12b-115	1375	622	487	0.863	0.06	0.103	0.005	0.0608	0.002	4	630	26
12b-116	271	147	124	0.969	0.08	0.112	0.006	0.0619	0.004	8	683	32
12b-117	371	249	198	0.930	0.08	0.109	0.005	0.0624	0.004	6	668	29
12b-118	185	121	89	0.890	0.08	0.105	0.005	0.0626	0.004	9	645	29
12b-119	350	310	235	0.885	0.07	0.106	0.005	0.0612	0.003	6	651	27
12b-120	232	147	124	0.930	0.09	0.108	0.005	0.0602	0.004	6	660	29
12b-121	2816	1302	1014	0.905	0.07	0.105	0.005	0.0614	0.003	4	650	29
12b-122	545	201	173	0.851	0.06	0.101	0.004	0.06	0.003	6	621	25
12b-123	473	429	84	0.840	0.13	0.099	0.008	0.062	0.01	11		
12b-124	176	105	94	0.826	0.07	0.100	0.004	0.0592	0.004	10	617	26
12b-125	200	85	77	0.845	0.08	0.100	0.004	0.0604	0.005	10	612	26
12b-126	11404	4353	3292	0.487	0.09	0.039	0.008	0.0897	0.004	29		
12b-127	404	72	64	0.822	0.09	0.099	0.005	0.058	0.005	11		
12b-128	548	228	205	0.787	0.07	0.095	0.005	0.0588	0.004	5	586	27
12b-129	674	364	321	0.819	0.07	0.098	0.005	0.06	0.005	6	604	27
12b-130	466	153	155	0.851	0.06	0.101	0.004	0.0599	0.003	6	623	26
12b-131	211	102	110	0.808	0.06	0.097	0.004	0.0606	0.003	7	594	25
12b-132	236	112	103	0.810	0.07	0.098	0.005	0.06	0.004	8	602	27
12b-133	145	49	54	0.890	0.13	0.104	0.007	0.065	0.011	14		
12b-134	248	155	144	0.846	0.09	0.097	0.006	0.0655	0.006	9	594	37
12b-135	454	64	71	0.816	0.08	0.098	0.005	0.0579	0.005	12		
12b-136	184	79	89	0.842	0.07	0.101	0.005	0.0599	0.004	8	621	26
12b-137	263	81	85	0.858	0.09	0.098	0.005	0.0617	0.004	8	601	31
12b-138	154	74	80	0.836	0.07	0.100	0.005	0.0601	0.004	9	615	26
12b-139	411	169	172	0.826	0.06	0.097	0.005	0.0627	0.004	6	598	30
12b-140	114	52	61	0.868	0.09	0.102	0.005	0.0635	0.006	11		
12b-141	191	84	94	0.848	0.06	0.101	0.004	0.0616	0.003	7	622	25
12b-142	406	155	174	1.000	0.13	0.115	0.006	0.0643	0.007	6	699	34
12b-143	520	170	169	0.812	0.06	0.100	0.004	0.0597	0.003	5	612	26
12b-144	531	210	178	0.839	0.06	0.100	0.004	0.0608	0.003	5	614	26
12b-145	343	107	106	0.793	0.07	0.098	0.005	0.0605	0.004	7	602	30
12b-146	229	87	89	0.845	0.07	0.102	0.005	0.06	0.004	6	623	27
12b-147	421	252	220	0.701	0.05	0.087	0.004	0.0591	0.003	7	537	23
12b-148	133	69	72	0.845	0.09	0.100	0.005	0.0627	0.006	11		
12b-149	645	179	169	0.795	0.07	0.097	0.005	0.058	0.004	5	595	26
12b-150	117	60	64	0.815	0.08	0.098	0.005	0.0588	0.005	10	602	27

32-1	24	35	22	0.920	0.16	9.747	0.408	0.063	0.011	26		
32-2	1177	279819	1E+05	0.821	0.04	10.917	0.322	0.0654	0.002	5	565	16
32-3	463	354	289	1.063	0.05	8.319	0.277	0.0648	0.003	5	732	23
32-4	110	116	142	0.814	0.07	10.194	0.384	0.0608	0.005	9	603	22
32-5	9400	228604	89914	0.536	0.03	15.576	0.558	0.0607	0.002	5	401	14
32-6	152	165	144	1.133	0.08	7.955	0.285	0.0649	0.004	5	763	26
32-7	234	278	756	12.620	0.67	1.957	0.103	0.1763	0.007	5	2624	33
32-8	135	180	114	0.744	0.06	10.661	0.318	0.0586	0.004	12		
32-9	142	138	119	1.096	0.06	8.078	0.248	0.0645	0.003	8	752	22
32-10	455	407	254	0.750	0.04	10.905	0.357	0.0612	0.003	5	566	18
32-11	70	82	66	0.721	0.05	11.074	0.356	0.0587	0.004	12		
32-12	139	313	1338	13.040	0.55	1.946	0.064	0.1822	0.005	4	2674	25
32-13	353	396	317	0.751	0.03	10.881	0.308	0.0595	0.002	5	566	15
32-14	266	208	165	0.738	0.04	11.086	0.32	0.0595	0.003	6	557	15
32-15	920	898	668	0.719	0.05	11.325	0.654	0.0603	0.005	4	546	30
32-16	269	172	177	1.071	0.05	8.190	0.241	0.0641	0.003	7	742	21
32-17	187	129	106	0.776	0.06	10.858	0.377	0.0628	0.004	7	568	19
32-18	47	17	18	1.025	0.08	8.562	0.293	0.0639	0.004	11		
32-19	68	14	15	0.925	0.07	9.234	0.307	0.0642	0.005	11		
32-20	109	59	166	5.100	0.27	3.058	0.094	0.1152	0.005	5	1864	26
32-21	128	127	454	11.100	0.48	2.227	0.069	0.1808	0.005	8	2658	25
32-22	83	32	32	1.122	0.08	7.955	0.259	0.0647	0.004	10	763	23
32-23	621	374	256	0.745	0.03	10.953	0.312	0.0602	0.002	5	563	15
32-24	257	195	150	0.761	0.05	10.881	0.426	0.0603	0.003	5	566	21
32-25	196	139	144	1.123	0.06	7.987	0.249	0.0657	0.003	7	760	23
32-26	152	97	353	11.400	1	2.049	0.126	0.17	0.007	7	2584	54
32-27	51	65	157	4.500	0.5	3.279	0.161	0.108	0.01	7	1734	94
32-28	26	71	56	0.850	0.23	9.653	0.82	0.061	0.013	17		
32-29	191	140	77	0.941	0.06	9.141	0.343	0.0626	0.004	7	669	24
32-30	96	140	348	4.280	0.22	3.344	0.134	0.1056	0.005	4	1721	48
32-31	66	42	35	0.738	0.07	10.941	0.359	0.0582	0.005	14		
32-32	55	38	36	0.820	0.12	10.215	0.563	0.0616	0.009	13		
32-33	116	61	67	1.051	0.07	8.418	0.283	0.0647	0.004	10	724	23
32-34	449	248	163	0.722	0.06	11.299	0.983	0.0655	0.004	11		
32-35	112	17	21	0.975	0.1	8.921	0.382	0.0655	0.007	9	685	28
32-36	8707	119216	72529	0.567	0.03	15.456	0.717	0.0634	0.001	7	404	18
32-37	378	161	159	0.849	0.05	9.833	0.3	0.0624	0.004	5	627	20
32-38	229	343	328	0.793	0.06	10.537	0.366	0.0614	0.004	8	586	20
32-39	198	153	145	0.729	0.04	11.136	0.322	0.0589	0.003	7	554	16

32-40	360	92	98	0.755	0.04	10.764	0.348	0.06	0.003	7	573	18
32-41	161	74	85	0.858	0.06	9.785	0.316	0.0612	0.004	9	627	19
32-42	314	118	106	0.847	0.06	9.833	0.329	0.0606	0.004	6	624	20
32-43	197	116	115	0.752	0.04	10.799	0.338	0.0598	0.002	6	572	17
32-44	153	96	94	0.781	0.05	10.493	0.352	0.0602	0.003	9	586	19
32-45	134	70	366	14.720	0.7	2.016	0.069	0.2154	0.007	10	2931	36
32-46	152	61	73	0.941	0.06	9.091	0.331	0.0636	0.003	7	672	23
32-47	200	219	249	0.762	0.05	10.753	0.358	0.0614	0.004	9	573	18
32-48	140	211	217	0.735	0.04	11.050	0.342	0.0593	0.003	8	558	17
32-49	402	54	53	0.750	0.07	11.050	0.403	0.0629	0.006	12		
32-50	479	481	2312	11.370	0.55	2.053	0.072	0.1736	0.005	3	2598	31
32-51	82	172	188	0.864	0.1	9.690	0.385	0.0614	0.006	11		
32-52	192	65	108	1.293	0.06	7.158	0.215	0.068	0.003	6	843	24
32-53	235	106	129	0.990	0.06	8.703	0.288	0.0633	0.003	6	701	22
32-54	389	107	163	1.125	0.06	7.974	0.331	0.067	0.003	4	761	30
32-55	184	33	127	6.160	0.32	2.755	0.091	0.1265	0.005	5	2057	37
32-56	366	297	323	0.791	0.04	10.493	0.352	0.0618	0.002	6	587	19
32-57	633	531	279	0.649	0.07	11.751	0.58	0.065	0.005	8	526	25
32-58	137	34	48	1.014	0.08	8.475	0.287	0.0628	0.005	8	719	23
32-59	56	64	79	0.823	0.06	10.142	0.37	0.0625	0.005	14		
32-60	90	22	29	0.948	0.06	9.083	0.289	0.0639	0.004	10	673	20
32-61	112	130	188	1.600	0.18	6.192	0.284	0.077	0.011	7	965	41
32-62	130	180	273	1.730	0.15	5.848	0.236	0.0705	0.005	7	1017	38
32-63	45	52	77	1.910	0.17	5.435	0.236	0.0736	0.007	10	1110	110
32-64	455	170	160	1.010	0.06	8.591	0.28	0.0618	0.003	5	710	22
32-65	170	185	135	0.806	0.06	10.246	0.42	0.0621	0.004	8	600	24
32-66	85	44	44	1.172	0.07	7.704	0.243	0.0656	0.004	9	787	23
32-67	118	38	30	0.979	0.07	8.795	0.286	0.0626	0.004	9	694	21
32-68	66	48	36	0.829	0.07	10.020	0.341	0.0615	0.005	14		
32-69	1232	82	42	0.799	0.04	10.277	0.486	0.0628	0.002	3	599	27
32-70	584	372	211	0.822	0.05	12.453	0.589	0.0752	0.003	15		
32-71	191	100	91	1.017	0.06	8.584	0.258	0.0635	0.003	7	710	20
32-72	42	28	93	8.750	0.54	2.309	0.091	0.142	0.01	7	2321	84
32-73	121	92	84	0.993	0.09	8.834	0.312	0.062	0.005	9	691	23
32-74	599	453	375	0.763	0.05	10.799	0.665	0.0611	0.003	4	571	34
32-75	266	301	269	0.781	0.04	10.604	0.315	0.0587	0.002	5	581	17
32-76	289	218	198	0.773	0.04	10.684	0.32	0.0601	0.003	5	576	17
32-77	162	105	333	5.560	0.33	2.890	0.117	0.1135	0.004	3	1884	40
32-78	132	64	82	1.250	0.2	7.391	0.328	0.066	0.009	7	818	34
32-79	97	54	69	0.960	0.13	8.826	0.428	0.0593	0.008	11		

32-80	117	38	43	0.865	0.06	9.823	0.338	0.0597	0.004	10	625	20
32-81	175	127	161	0.771	0.06	10.718	0.368	0.0604	0.004	10	575	19
32-82	229	90	110	0.798	0.06	10.246	0.399	0.0582	0.004	7	600	22
32-83	1998	513	381	0.607	0.03	20.877	1.09	0.0891	0.003	28		
32-84	286	517	519	0.749	0.05	13.175	0.521	0.0726	0.004	13		
32-85	664	265	231	0.774	0.04	11.765	0.595	0.0644	0.003	7	526	25
32-86	86	69	95	0.727	0.05	10.892	0.368	0.0576	0.004	11		
32-87	99	93	125	0.792	0.06	10.582	0.258	0.0588	0.004	12		
32-88	272	158	219	0.771	0.04	10.718	0.356	0.0586	0.003	6	575	19
32-89	245	72	114	0.833	0.06	9.990	0.309	0.0599	0.004	6	615	18
32-90	219	126	142	0.901	0.08	9.381	0.431	0.0602	0.005	4	653	28
32-91	44	50	69	0.820	0.12	10.070	0.497	0.0604	0.009	14		
32-92	205	35	51	0.873	0.05	9.756	0.286	0.0606	0.003	9	629	17
32-93	116	61	81	0.830	0.06	10.204	0.302	0.0608	0.004	11		
32-94	100	111	144	0.798	0.06	10.515	0.354	0.0585	0.004	10	586	19
32-95	167	70	92	0.817	0.06	10.331	0.32	0.0588	0.003	8	597	17
32-96	76	60	77	0.788	0.07	10.604	0.416	0.0582	0.005	12		
32-97	224	116	139	0.800	0.05	10.309	0.393	0.0595	0.004	8	597	22
32-98	291	278	314	1.075	0.07	9.200	0.508	0.0709	0.003	9	668	34
32-99	154	235	266	0.788	0.06	10.616	0.417	0.0598	0.004	9	580	22
32-100	9335	10740	1255	0.327	0.06	75.188	18.09	0.217	0.016	66		
32-101	2027	1261	622	0.678	0.04	21.008	1.059	0.1024	0.002	35		
32-102	419	179	134	0.881	0.04	9.569	0.275	0.0608	0.002	4	641	18
32-103	65	74	179	6.530	0.4	2.681	0.108	0.1248	0.007	6	2045	44
32-104	226	287	194	0.990	0.17	9.727	0.474	0.0686	0.01	12		
32-105	1008	1061	1117	3.250	0.17	5.294	0.255	0.1218	0.003	26		
32-107	175	344	209	0.805	0.05	10.277	0.296	0.0589	0.003	7	599	17
32-108	2793	546	418	0.500	0.03	29.240	1.624	0.1062	0.004	37		
32-109	114	38	25	0.813	0.06	10.194	0.374	0.0587	0.004	10	603	21
32-110	130	245	140	0.839	0.05	10.101	0.337	0.0606	0.004	7	609	19
32-111	320	610	205	0.655	0.06	12.151	0.546	0.0576	0.004	8	510	22
32-112	72	35	30	1.210	0.15	7.645	0.316	0.0683	0.008	13		
32-113	50	52	35	0.841	0.07	10.020	0.361	0.0617	0.005	12		
32-114	72	44	27	0.780	0.11	10.834	0.516	0.064	0.01	17		
32-115	222	230	141	0.802	0.06	10.235	0.43	0.0574	0.004	6	601	24
32-116	155	185	133	0.859	0.05	9.852	0.311	0.0608	0.003	7	623	19
32-117	47	49	36	0.929	0.1	9.302	0.476	0.0626	0.007	15		
32-118	244	86	79	1.151	0.06	7.813	0.238	0.0652	0.003	7	776	22
32-119	355	264	455	4.850	0.21	3.416	0.109	0.1205	0.003	8	1965	25
32-120	185	220	171	0.834	0.05	10.163	0.341	0.0615	0.004	9	605	20

32-121	474	300	214	0.784	0.04	10.482	0.297	0.0602	0.002	6	587	16
32-122	228	179	144	0.875	0.06	9.560	0.356	0.0609	0.003	6	641	23
32-123	268	246	164	0.789	0.04	10.616	0.338	0.0617	0.003	6	580	17
32-124	152	170	110	0.833	0.08	10.183	0.342	0.0623	0.005	10	603	19
32-125	145	45	37	0.935	0.05	9.208	0.271	0.062	0.003	7	664	18
32-126	920	1521	1693	2.720	0.16	13.870	0.731	0.285	0.02	92		
32-127	231	444	343	0.781	0.05	10.582	0.336	0.0595	0.003	7	583	17
32-128	232	389	202	0.695	0.06	11.682	0.45	0.0591	0.005	8	529	20
32-129	83	27	21	0.842	0.07	9.960	0.347	0.0605	0.004	11		
32-130	288	312	235	0.804	0.04	10.384	0.345	0.0596	0.002	6	592	19
32-131	200	73	67	0.782	0.04	10.593	0.314	0.06	0.003	7	581	16
32-132	391	178	251	1.423	0.07	6.720	0.23	0.0708	0.002	5	894	28
32-133	26	77	65	0.850	0.1	10.194	0.655	0.0651	0.007	16		
32-134	416	287	258	0.785	0.04	10.395	0.346	0.0589	0.002	6	592	19
32-135	82	92	296	8.530	0.97	2.364	0.156	0.145	0.013	6	2318	77
32-136	134	19	24	1.150	0.14	7.831	0.294	0.0651	0.009	8	775	27
32-137	421	98	103	0.882	0.04	9.615	0.296	0.0621	0.002	5	638	18
32-138	156	204	200	0.807	0.04	10.204	0.323	0.0603	0.003	8	602	18
32-139	107	88	87	0.890	0.1	9.569	0.44	0.0629	0.006	9	640	28
32-140	191	131	128	0.830	0.05	9.921	0.315	0.059	0.003	8	619	19
32-141	143	74	70	0.737	0.04	10.846	0.329	0.0582	0.003	8	568	17
32-142	584	346	505	1.300	0.12	7.143	0.434	0.0681	0.006	4	845	48
32-143	431	113	119	0.856	0.04	9.671	0.318	0.0599	0.002	6	634	20
32-144	166	55	57	0.910	0.11	9.311	0.485	0.0657	0.006	9	657	33
32-145	394	222	199	1.009	0.05	8.569	0.279	0.0631	0.002	6	713	22
32-146	182	77	85	0.790	0.12	10.549	0.734	0.0606	0.008	6	584	39
32-147	31	14	13	0.790	0.11	10.627	0.486	0.0611	0.008	22		
32-148	106	57	68	1.057	0.06	8.251	0.245	0.063	0.003	7	738	21
32-149	156	133	127	0.759	0.05	10.776	0.314	0.0601	0.003	9	572	16
32-150	63	32	30	0.781	0.06	10.460	0.339	0.0598	0.005	13		